Building Simulation 2009
Eleventh International IBPSA Conference
Glasgow, Scotland
July 27-30, 2009

TESTING AND VALIDATION OF SIMULATION TOOLS OF HVAC MECHANICAL EQUIPMENT INCLUDING THEIR CONTROL STRATEGIES PART III: VALIDATION OF AN AIR-COOLED CHILLER MODEL

Vincent Lemort[1], Jean Lebrun[1], and Clemens Felsmann[2]
[1]Thermodynamics Laboratory, University of Liège, Belgium
[2]Institute of Thermodynamics and Building Systems Engineering, Technical University of Dresden, Germany

ABSTRACT

This paper presents a semi-empirical steady-state model of an air-cooled water chiller. The first part of the paper shows how the model is built by associating a scroll compressor and two heat exchanger sub-models.

The second part of the paper presents the parameters identification process based on published manufacturer data (for the compressor and the whole chiller models). The only encountered difficulty is the characterization of the fan control model, since information is lacking to identify its parameters.

The third part of the paper presents results of an experimental investigation carried out on the same chiller integrated into an existing cooling plant. A detailed analysis of the experimental data allowed a better understanding of the chiller's operation and a better identification of the model's parameters (such as the models of the fan control and of the compressor staging control). Moreover, a simple but realistic model of the condenser hot gas by-pass was introduced. As a result, deviations between predictions by the model and the experimental data were considerably reduced.

The model is finally found to predict the total cooling energy and the total electrical consumption over a long-term simulation period with a very good accuracy.

INTRODUCTION

An accurate simulation of chilled water systems is welcome at main stages of HVAC system life cycle: design, evaluation, commissioning and management. This paper focuses on the modeling of an air-cooled water chiller that is a major component of a chilled water system.

The underlying work was carried out in the frame of a project of the International Energy Agency (Felsmann, 2008). The goal of this project was to undertake pre-normative research to develop testing methods of building energy simulation tools. A part of this project focused on the modeling and the simulation of the performance of certain components that are part of a chilled and/or a heating water system.

The chiller semi-empirical model presented in this paper is described by physical equations involving a limited number of parameters. The latter can be identified on the basis of performance measurements or manufacturer data. Semi-empirical models lay between empirical models (that are based on polynomial regressions) and deterministic models (that are comprehensive models based on heat, mass and momentum transfers and require the exact characteristics of the components). Semi-empirical models are less time-consuming and more numerically robust than deterministic models. Hence, they are easier to integrate into the modeling of a larger system. Moreover, unlike empirical models, semi-empirical models allow the extrapolation of the component's performance beyond the range of data used to identify their parameters (Jin and Spitler, 2002a).

The identification of the parameters of the chiller model and its validation will be achieved in two steps: first on the basis of published manufacturer data and then on the basis of experimental results. Manufacturer data is often the only source of information available to model HVAC components. Some information is usually lacking to accurately validate the model and assumptions and idealizations must be proposed. The experimental investigation carried out on the chiller must allow checking these assumptions, characterizing better the chiller and improving its modeling.

MODELING OF THE CHILLER

The models proposed by Bourdhouxe et al. (1994) are among the first semi-empirical models of chillers. The authors presented well documented models with reciprocating, screw and centrifugal compressors, as well as parameter determination procedures for the models of the compressor and of the whole chiller (in both full- and part-load operation). More recently, Jin and Spitler proposed a semi-empirical model for a water-to-water chiller with scroll compressors (Jin and Spitler, 2002a) and with reciprocating compressors (Jin and Spitler, 2002b). They showed how the model's parameters can be identified based on published manufacturer data.

The model proposed here is similar to the model developed by Jin and Spitler (2002), but accounts for three control processes: condenser fan speed, hot gas by-pass and compressors staging.

The chiller model associates the sub-models of a scroll compressor, an evaporator and a condenser. It can be conventionally described by the information flow diagram presented in Figure 1:

I) For given supply conditions and exhaust pressure and for a given number of compressors, running at constant rotational speed, the compressor model imposes the refrigerant mass flow rate through the cycle.
II) For given air mass flow rate and supply temperature, the condenser model imposes the condensing pressure. The liquid subcooling at the condenser exhaust is here imposed. It is actually a function of the refrigerant charge in the cycle, and, in a more detailed representation, could be predicted by introducing void fraction models for the heat exchangers.
III) The expansion valve model assumes that expansion is isenthalpic, which imposes the vapor enthalpy at the evaporator supply. With a "perfect control" assumption, it also imposes the vapor superheat at evaporator exhaust.
IV) For given water flow rate and temperature, the evaporator model imposes the evaporating pressure.

In Figure 1, none of the three control processes already mentioned (fan speed, condenser by-pass and compressor staging) is yet represented. These processes will be later introduced in the modeling.

Scroll compressor model

As indicated in Figure 2, the modeling of the compressor assumes that the evolution of the refrigerant is decomposed into the following steps (Winandy et al., 2002): supply heating-up (su → su,1); mixing with the internal leakage (su,1 → su,2); isentropic compression (su,2 → in); adiabatic and isochoric compression (in → ex2); exhaust pressure drop (ex,2 → ex,1); exhaust cooling-down (ex,1 → ex).

The distinction between isentropic and isochoric compressions allows describing the over- and under-compression losses associated with the fixed built-in volume ratio of the compressor. The internal compression power is given by the following equation:

$$\dot{W}_{in} = \dot{M}_{in}\left(\left(h_{r,in,cp} - h_{r,su2,cp}\right) + v_{r,in,cp}\cdot\left(P_{r,ex2,cp} - P_{r,in,cp}\right)\right) \quad (1)$$

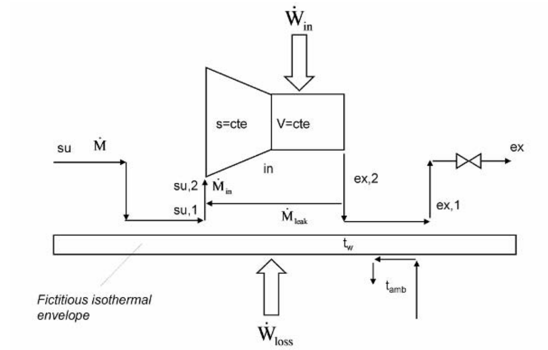

Figure 2 Schematic representation of the scroll compressor model

The compressor consumption is the summation of the internal power and of the electro-mechanical losses. The latter can be decomposed between constant losses and losses proportional to the internal power.

$$\dot{W}_{cp} = (1+\alpha)\dot{W}_{in} + \dot{W}_{loss,0} \quad (2)$$

The refrigerant flow rate displaced by the compressor is given as a function of the internal and leakage flow rates by:

$$\dot{M}_{r,cp} = \dot{M}_{in} - \dot{M}_{leak} = \frac{\dot{V}_{s,cp}}{v_{r,su2,cp}} - \dot{M}_{leak} \quad (3)$$

The model necessitates 9 parameters: the compressor swept volume, its built-in volume ratio $r_{v,in}$, a lumped leakage area A_{leak}, the constant electro-mechanical loss term, a factor of proportionality α for the electro-mechanical loss proportional to the internal power, a suction heat transfer coefficient AU_{su}, an exhaust heat transfer coefficient AU_{ex}, a heat transfer coefficient between the compressor and the ambient AU_{amb} and a fictitious diameter d_{ex} of the exhaust opening.

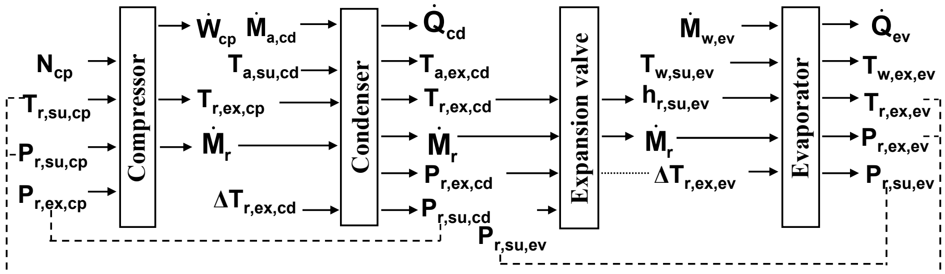

Figure 1 Schematic representation of the chiller model

Evaporator and condenser models

The basic modeling of the evaporator and the condenser consists in assuming that the heat exchanger is semi-isothermal, with the constant temperature equal to the saturation temperature. The single-phase zones of the heat exchanger are neglected and the model reduces to a one-zone heat exchanger. This assumption is acceptable for the evaporator of a chiller, since it presents a large two-phase zone and a small single-phase (superheating) zone.

In order to be more accurate in the condenser modeling, the condensing temperature can be defined as the weighted average of the actual temperatures occurring in the three zones (single-phase desuperheating, two-phase condensation and single-phase undercooling):

$$\bar{t}_{cd} = \left\{ (h_{r,su,cd} - h_{r,su,cd,tp}) \left[\frac{T_{r,su,cd} + T_{cd}}{2} \right] + (h_{r,su,cd,tp} - h_{r,ex,cd,tp}).T_{cd} + (h_{r,ex,cd,tp} - h_{r,ex,cd}) \left[\frac{T_{r,ex,cd} + T_{cd}}{2} \right] \right\} \Big/ \left(h_{r,su,cd} - h_{r,ex,cd} \right) \quad (4)$$

For both heat exchangers, the overall heat transfer coefficient AU is computed by associating 3 heat transfer resistances in series:

$$\frac{1}{AU_{\substack{ev\\cd}}} = R_{\substack{r,ev\\r,cd}} + R_{\substack{m,ev\\m,cd}} + R_{\substack{w,ev\\a,cd}} \quad (5)$$

In order to account for the dependency of the heat transfer coefficient with the refrigerant and secondary fluids flow rates, the convective resistance is assumed to vary with the mass flow rate according to

$$R = R_n \cdot \left(\frac{\dot{M}_n}{\dot{M}} \right)^m \quad (6)$$

A value of 0.8 (turbulent regime) of the exponent m was considered for the refrigerant- and glycol water-sides and a value of 0.6 (laminar regime) for the air side.
The evaporating and condensing powers are computed by using the ε-NTU method. For the condenser, it gives:

$$\dot{Q}_{cd} = \left(1 - exp\left(\frac{-AU_{cd}}{\dot{C}_{a,cd}} \right) \right) \dot{C}_{a,cd} \left(\bar{t}_{cd} - t_{a,su,cd} \right) \quad (7)$$

Fan control model

Condenser fan motors are automatically cycled in response to the condenser pressure by a standard method of control of the condensing pressure (or temperature). The second fan cycles in order to maintain the condensing pressure, which allows the unit to run at low ambient air temperature down to 1.7°C. The first fan modulates its motor speed in response to condenser pressure, which allows the unit to operate down to -18°C.

This control can be described by the following set of equations. The fan control variable is proportional to the difference between the actual condensing temperature and the condensing temperature set point

$$X_{contr,fan} = MAX(0, gain_{fan}(t_{cd} - t_{cd,set})) \quad (8)$$

The air volume flow rate through the condenser is adjusted by means of the control variable:

$$\dot{V}_{a,cd,set} = \dot{V}_{a,cd,\min} + \left(\dot{V}_{a,cd,\max} - \dot{V}_{a,cd,\min} \right) X_{contr,fan} \quad (9)$$

However, the air flow rate is limited by a maximal value:

$$\dot{V}_{a,cd} = MIN\left(\dot{V}_{a,cd,set}, \dot{V}_{a,cd,\max} \right) \quad (10)$$

The gain and the condensing set point temperature in Equation (8) are two parameters to identify.

The chiller electrical consumption is the summation of the electrical consumption of the compressors, the fans and the auxiliaries (crankcase heater, controller):

$$\dot{W}_{tot} = \dot{W}_{cp,tot} + \dot{W}_{fan} + \dot{W}_{aux} \quad (11)$$

PARAMETERS IDENTIFICATION

The investigated chiller consists of a set of two air-cooled condensers, two hermetic scroll compressors in tandem, one brine-heated evaporator and a hot gas by-pass (Figure 3). Its nominal cooling capacity is 34.3 kW in ARI Conditions (ARI Standard 550/590, 1998) for 460 V, 3-phase, 60 Hz regime. These conditions correspond to a 35°C air temperature at condenser supply, a glycol water flow rate of 1.51 l/s (glycol water is here a 25% in mass aqueous solution of propylene glycol) and a glycol water temperature of 6.7°C at evaporator exhaust. Full load COP (Coefficient of Performance) is 2.84 and part load COP is 3.58 (including fan and auxiliaries consumption).

The identification of the parameters of the model is achieved in two steps:
1) The parameters of the compressor model are first identified, according to the compressor performance data.

2) The parameters of the evaporator and the condenser models are then identified, according to chiller performance data.

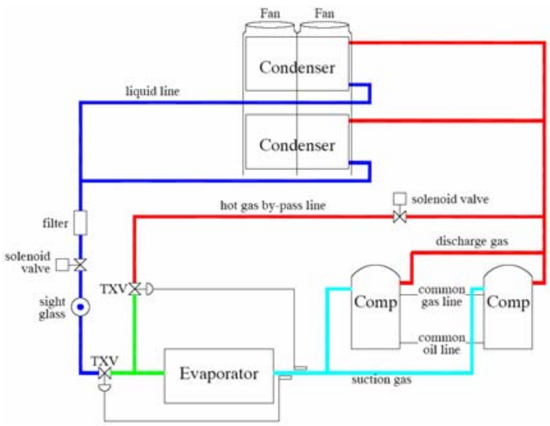

Figure 3 Air-cooled chiller refrigerant circuit

Parameters of the scroll compressor model

The compressor cooling capacity, its electrical consumption and the corresponding refrigerant mass flow rate it displaces are given by the manufacturer at 57 operating points, as a function of the evaporating and the condensing temperatures, for given values of the subcooling at condenser exhaust and for the superheat at evaporator exhaust.

The parameters of the compressor model are tuned in order to bring the values of the refrigerant mass flow rate, the power consumption and the cooling capacity predicted by the model as close as possible to the values announced by the manufacturer. Figure 4 shows that the evaporating and condensing temperatures as well as the compressor suction superheat and the condenser subcooling are input variables of the model, while the model calculates the mass flow rate, the power consumption, the cooling and the heating capacities.

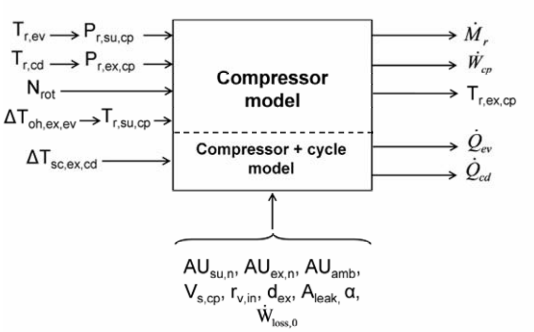

Figure 4 Information diagram of the compressor model

The identified parameters are given in the information diagram of the chiller model represented in Figure 11. Predictions by the model are compared to the values announced by the manufacturer in Figure 5 for the refrigerant mass flow rate and in Figure 6 for the overall isentropic effectiveness.

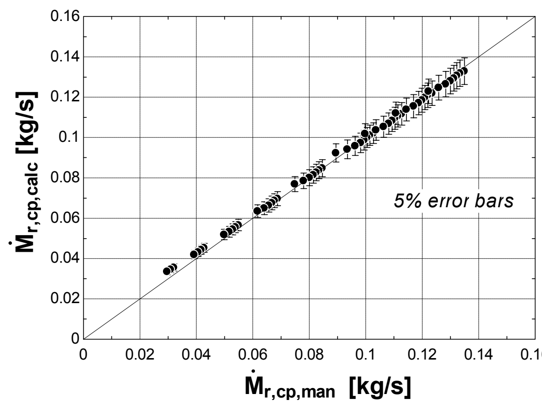

Figure 5 Prediction of the displaced refrigerant mass flow rate (compressor model)

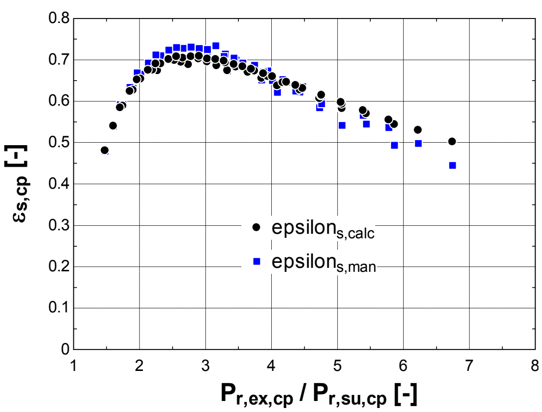

Figure 6 Prediction of the compressor isentropic effectiveness (compressor model)

Parameters of the heat exchanger models

Thirty performance points are given by the chiller manufacturer. Cooling capacities and corresponding electrical consumptions are presented as functions of the water temperature at evaporator exhaust ($T_{w,ex,ev}$) and of the air temperature at condenser supply ($T_{a,su,cd}$), according to standards (ARI Standard 550/590, 1998).

The parameters of the condenser and the evaporator models (three resistances and two nominal flow rates) are identified on the basis of one of the 30 points (the closest to the ARI rating conditions) by imposing the cooling capacity and the compressor consumption calculated by the model equal to the values announced by the manufacturer.

This only represents two equations for a total of six resistances to be identified. The required additional four relationships are found by assuming that the refrigerant-side, metal and secondary fluid (air or water) are equal among themselves in reference conditions.

The chiller investigated here comprises two fans. The condenser nominal airflow rate given by the manufacturer is 23700 m^3/h (defined conventionally at condensers exhaust).

Performances announced by the manufacturer do not allow identifying the parameters of the fan control model: the best agreement is found by assuming that the fans are working at their nominal air flow rate. The identified constant fan consumption is 1100 W.

The agreement between predictions by the model and the measurements is shown in Figure 7 for the COP.

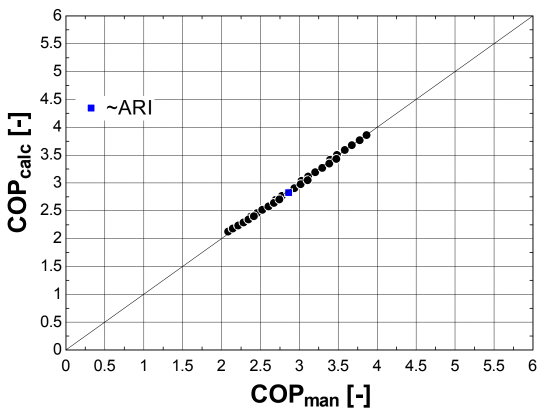

Figure 7 Prediction of the chiller COP (chiller model)

EXPERIMENTAL INVESTIGATION

Experimental data was collected on an existing chilled water system, installed in a small office building (the Energy Resource Station located at Ankeny, Iowa, USA). The system comprises an air-cooled scroll compressor chiller, a cooling coil inside an air handling unit and a hydraulic network including a circulating pump and a mixing valve.

The experiment was conducted from August 8 to 23, 2006 and measurements were collected minute by minute. Chilled water is an aqueous solution of propylene glycol 18% in volume.

The chilled water temperature at the chiller exhaust ($T_{w,ex,ev}$) is set at 4.4°C and the chilled water pump speed is kept constant in mass (glycol water flow rate was around 5.5m^3/h).

The following variables are the only ones actually measured: compressor and fan electrical consumptions, compressor supply and exhaust pressures, glycol water temperatures at evaporator supply and exhaust, glycol water flow rate and air temperatures at the condenser supply and exhaust.

Air and refrigerant flow rates were not measured. The former is estimated by expressing the energy balance across the chiller and the latter is estimated by considering the compressor as a flow meter.

The chiller was simulated over the entire experimental domain, with the model parameters previously identified based on published manufacturer data. The total cooling energy (integration of the cooling power over the simulation period) predicted by the model was found as 30% higher than the measured cooling energy (Figure 15). In order to understand the reasons of this discrepancy and probably to allow a better identification of the chiller model parameters, 10 quasi-steady state points were extracted from experimental data. These points correspond to quasi-stabilized air and water temperatures.

Parameters of the fan control model

The analysis of these points allowed identifying the parameters of the condenser fan control model. Figure 8 compares the condenser air flow rates determined from measurements and predicted by the model, respectively. This figure shows that the model is able to predict the trend for the control of the fan (for the considered period, only one fan was working): the fan is reducing its speed under a threshold close to 1600 kPa. The same comparison is given in Figure 9 for the fan electrical consumption. The fan electrical consumption is found to vary quasi linearly with the air volume flow rate.

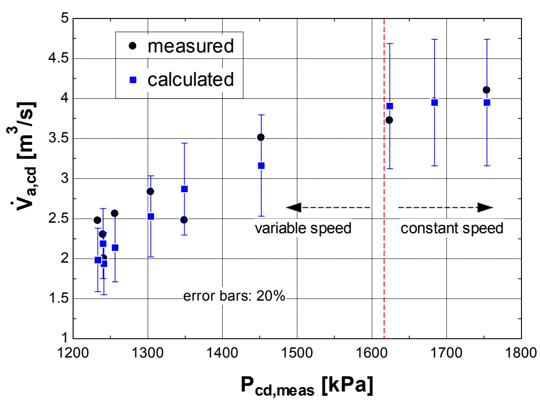

Figure 8 Prediction of the condenser air flow rate (chiller model)

Condenser hot gas by-pass control

In order for the model to predict with a good agreement the cooling power, a description of the hot gas by-pass control had to be introduced in the modeling. This system prevents evaporator frosting and excessive cycling at low load operation, and maintains the refrigerant velocity in the evaporator high enough for proper oil return to the compressor.

The refrigerant mass flow rate through the condenser is given as function of the refrigerant flow rate displaced by the compressor by:

$$\dot{M}_{r,cd} = (1 - X_{BP})\dot{M}_{r,cp} \tag{12}$$

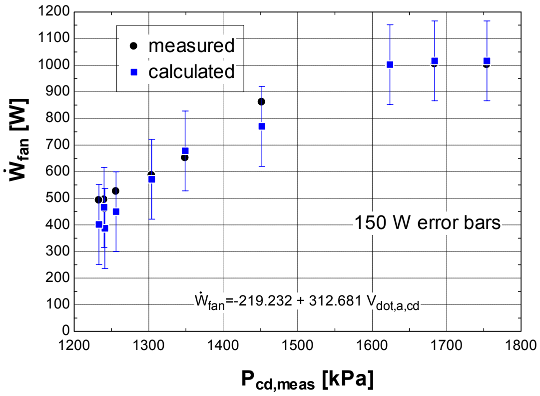

Figure 9 Prediction of the fan electrical consumption (chiller model)

The control of the by-pass is described by means of a hypothetical quasi-static model similar to the fan control model. Equations governing its modeling are given hereunder. The by-pass control variable is supposed to be proportional to the difference between the evaporating pressure (compressor supply pressure) set point and the actual evaporating pressure.

$$X_{contr,BP} = MAX(0, gain_{BP}(P_{ev,set} - P_{ev})) \tag{13}$$

The fraction of by-pass refrigerant X_{BP} is defined as follows:

$$X_{BP,set} = X_{BP,\min} + \left(X_{BP,\max} - X_{BP,\min}\right)X_{contr,BP} \tag{14}$$

$$X_{BP} = MIN\left(X_{BP,set}, X_{BP,\max}\right) \tag{15}$$

The evaporator was fed at constant glycol water flow rate, which didn't enable to identify separately the water-side and the metal resistances. Identified resistances are given in Figure 11. This figure also indicates the input variables (air supply dry and wet bulb temperatures, water flow rate, water supply temperature and number of working compressors) and the outputs variables (the chiller consumption, its COP and the air and water temperatures at the exhaust of the condenser and evaporator).

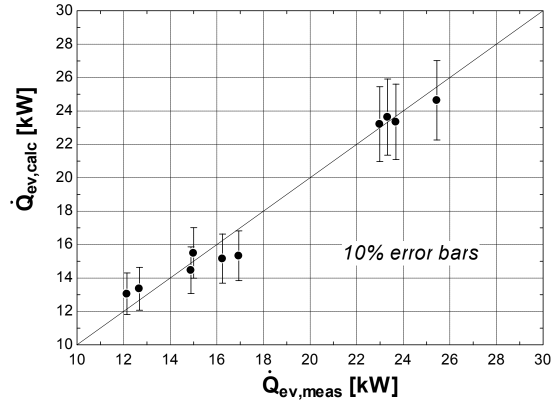

Figure 10 Prediction of the cooling power (chiller model)

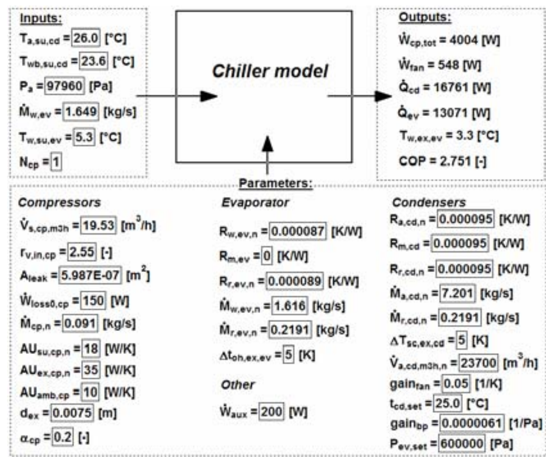

Figure 11 Information diagram of the chiller model

Other chiller control process

The chiller is controlled by switching on/off one or two compressors depending on the evaporator leaving water temperature. This control is represented in Figure 12, where "stage 1" indicates that the lead compressor cycles on/off and "stage 2" indicates that the lag compressor cycles on/off. The dead band is automatically set of 60% of the difference between the entering temperature and the leaving temperature set point:

$$\Delta T_{DB} = 0.6 \cdot (T_{w,su,ev} - T_{w,ex,ev,set}) \tag{16}$$

The start of the lead compressor is determined by the dead band ΔT_{DB} and settings. ΔT_{start} is the number of degrees above the evaporator exhaust water temperature set point that determines when the lead compressor starts.

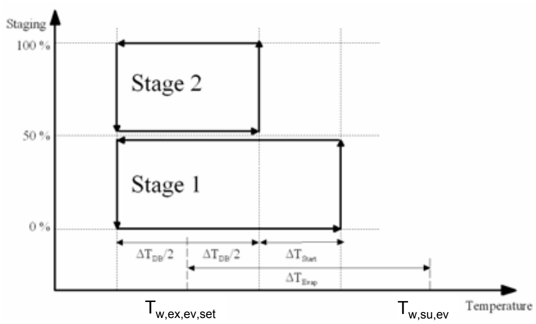

Figure 12 Chiller control scheme

For a warm start-up the lead compressor will start at any temperature above $T_{w,ex,ev,set}+0.5\Delta T_{DB}+\Delta T_{start}$. The lag will start after 240 sec. The chilled water temperature will begin to be pulled down. At $T_{w,ex,ev,set}-0.5\Delta T_{DB}$ the lag compressor will shut off. If the temperature climbs above $T_{w,ex,ev,set}-0.5\Delta T_{DB}$ within 30 sec, the lead compressor will remain on. This would be normal operation. If for some reason the temperature does not rise, the lead compressor will also shut off. The lead compressor will start again when the chilled water temperature reaches $T_{w,ex,ev,set}+0.5\Delta T_{DB}+\Delta T_{start}$.

This description of the control is compared to experimental data in Figure 13 representing the cooling power as a function of the evaporator leaving water temperature.

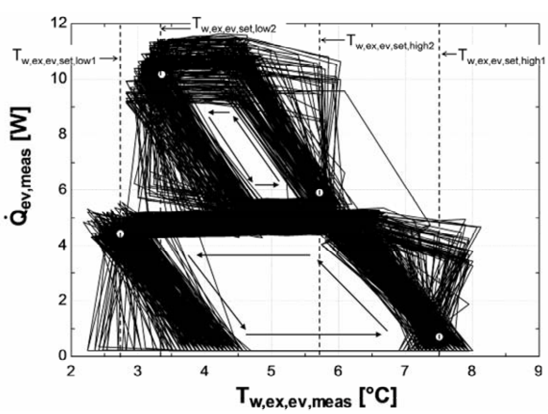

Figure 13 Control map of the chiller

According to this figure, the staging of the compressors can be described by Equations (17).

These equations give the number of working compressors $N_{cp}(i)$ at the current time step as function of the number of working compressors $N_{cp}(i-1)$ at previous time step and of the derivative with time of the leaving water temperature $dT_{w,ex,ev}(i-1)/dt$ at the previous time step.

In the expression if(A, B, X, Y, Z) : if A<B, the function will return a value equal to the value supplied for X; if A=B, the function will return the value of Y; if A>B, the function will return the value of Z.

$$\begin{cases} N_{cp}(i) = if\begin{pmatrix} N_{cp}(i-1), 0, N_{cp,0}, N_{cp,0}, \\ if\left(N_{cp}(i-1), 1, N_{cp,1}, N_{cp,1}, N_{cp,2}\right) \end{pmatrix} \\ N_{cp,0} = if\left(T_{w,ex,ev}(i-1), T_{w,ex,ev,set,high1}, 0,0,1\right) \\ N_{cp,1} = if\left(dT_{w,ex,ev}(i-1)/dt, 0, N_{cp,11}, N_{cp,11}, N_{cp,12}\right) \\ N_{cp,11} = if\left(T_{w,ex,ev}(i-1), T_{w,ex,ev,set,low1}, 0,0,1\right) \\ N_{cp,12} = if\left(T_{w,ex,ev}(i-1), T_{w,ex,ev,set,high2}, 1,1,2\right) \\ N_{cp,2} = if\left(T_{w,ex,ev}(i-1), T_{w,ex,ev,set,low2}, 1,1,2\right) \end{cases} \quad (17)$$

Long term simulation

The chiller is simulated over the whole experimental data (August 8-23, minute by minute). The input variables of the simulation are the glycol water and the air temperatures at the evaporator and condenser supply and the glycol water flow rate.

A first simulation is carried out with the number of working compressors imposed (which assumes a perfect control of the chiller). The system is then simulated after introducing the model of the compressor staging control previously described. Comparison between the results of both simulations indicates the ability of the model to represent the chiller control.

Figure 14 represents the time evolution of the chiller cooling power measured and predicted by the model (accounting for the chiller control). This figure shows that the model is able to predict the general trend for the staging of the compressors.

Figure 15 compares the total cooling and electrical energies (integration of the cooling power and electrical consumption over the entire simulation period) measured and predicted by the chiller model accounting or not for the description of the hot gas by-pass and compressor staging controls. These results show that the simulation model, with the description of the different control processes, is able to predict the performance of the chiller with a very good accuracy.

CONCLUSION

At least in the case considered here, the information published by the manufacturers is not detailed enough for an accurate identification of the parameters of HVAC component models. Lacking information has to be replaced by rational assumptions. This was illustrated in this paper in the case of an air-cooled water chiller.

Experimental data, collected on a real installation, allowed checking these assumptions and identifying with a much better accuracy the parameters of the chiller model. This is the case of the parameters of the fan control model. The latter is now able to predict the air flow rate through the condenser and the fan electrical consumption with a good accuracy.

The chiller simulation model was also improved. First, a simple but realistic model of the condenser hot gas by-pass was added, which yields much better results for the prediction of the cooling capacity. Then, the modeling of the staging control of the compressors was introduced. This model predicts with a good accuracy the control of the chiller.

The chiller model was finally tested over long-term simulation and was found to give very accurate results for both the predictions of the cooling and electrical energies.

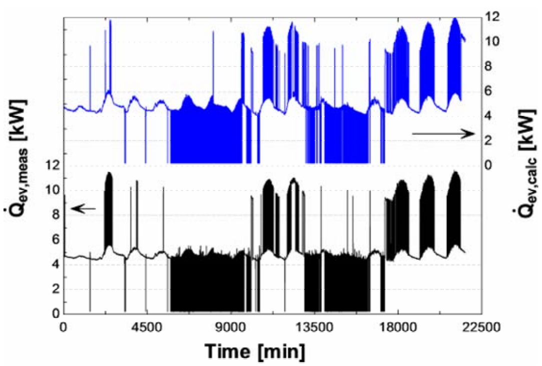

Figure 14 Time evolution of the chiller measured and predicted cooling power

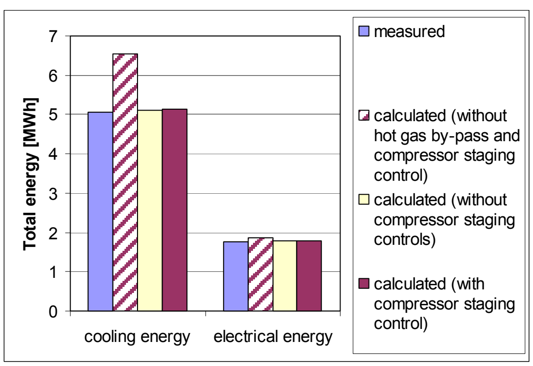

Figure 15 Total cooling and electrical energies over the entire simulation period

NOMENCLATURE

A,	Area, m^2
AU,	Heat transfer coefficient, W/K
c	Specific heat, J/kg-K
d	Diameter, m
h	Specific enthalpy, J/kg
$\dot{M}$	Mass flow rate, kg/s
N	Number, -
$\dot{Q}$	Heat transfer rate, W
R	Heat transfer resistance, K/W
t	Temperature, °C
$\dot{V}$	Volume flow rate, m^3/s
$\dot{W}$	Power, W
X	Control variable, -

Subsctript

0	Constant	man	Manufacturer
a	Air	meas	Measured
amb	Ambient	n	Nominal
aux	Auxiliaries	p	Isobaric
bp	By-pass	r	Refrigerant
calc	Calculated	s	Isentropic
cd	Condenser	set	Set point
cp	Compressor	sh	Superheat
ex	Exhaust	su	Supply
ev	Evaporator	tot	Total
in	Internal	tp	Two-phase
leak	Leakage	w	Envelope, water
m	Metal	wb	Wet bulb

REFERENCES

ARI Standard 550/590. 1998. Water Chilling Packages using the Vapor Compression Cycle, Air-Conditioning and Refrigeration Institute, 4301 North Fairfax Drive, Suite 425, Arlington, VA 22203, U.S.A.

Bourdouxhe, J-P H., M. Grodent, J.J. Lebrun, C. Saavedra, and K.L. Silva. 1994. A toolkit for primary HVAC system energy calculation—Part 2: Reciprocating chiller models. ASHRAE Transactions 100(2): 774-786.

Felsmann, C. 2008. Mechanical Equipment & Control Strategies for a Chilled Water and a Hot Water System. A Report for the International Energy Agency's SHC Task 34/ECBCS Annex 43 Subtask D.

Jin, H., and J.D. Spitler. 2002a. A Parameter Estimation Based Model of Water-to-Water Heat Pumps for Use in Energy Calculation Programs, ASHRAE Transactions 2002, Vol 108, Part 1.

Jin, H., and J. Spitler. 2002b. Parameters Estimation Based Model of Water-to-Water Heat Pumps with Scroll Compressors and Water/Glycol Solutions, Proceedings of the Sixth International Conference on System Simulation in Buildings.

Winandy, E., C. Saavedra, and J. Lebrun. 2002. Experimental analysis and simplified modelling of a hermetic scroll refrigeration compressor, Applied Thermal Engineering 22: 107-120.